31st Annual International Conference of the IEEE EMBS
Minneapolis, Minnesota, USA, September 2-6, 2009

Multidimensional AM-FM Models and Methods for Biomedical Image Computing

M.S. Pattichis, *Senior Member, IEEE*

***Abstract*— This paper provides an overview of multidimensional AM-FM methods for analyzing medical images and videos. Over the last decade, several new AM-FM demodulation methods have been developed. We provide a discussion of what many of these methods share in common, and give some details on recent, Hilbert-based approaches.**

Medical image applications range from medical image segmentation, resolution enhancement, classification, reconstruction to new methods for video motion estimation. A brief summary of suggestions for future work in this area is also given.

I. Introduction

Multi-dimensional Amplitude-Modulation Frequency-Modulation (AM-FM) models and methods provide us with powerful, image and video decompositions that can effectively describe non-stationary content. They represent an extension to standard Fourier analysis, where we allow both the amplitude and the phase functions to vary spatially over the support of the image, following changes in local texture and brightness.

To explain some of the advantages of AM-FM methods, we begin with the basic AM-FM model. In the 2D model, we expand an input image $I(x,y)$ into a sum of AM-FM harmonics using:

$$I(x,y)=\sum_{n=1}^{N} a_n(x,y)\cos\phi_n(x,y) \qquad (1)$$

Where $a_n(x,y)$ denote slowly-varying instantaneous amplitude (IA) functions, $\phi_n(x,y)$ denote the instantaneous phase (IP) components, and $n=1,2,\ldots,N$ indexes the different AM-FM harmonics. In (1), we have that the n-th AM-FM harmonic represented by $a_n(x,y)\cos\phi_n(x,y)$.

In terms of texture features, for each phase function, we associate the instantaneous frequency (IF) vector field defined by $\nabla\phi_n(x,y)$. Here, the AM-FM demodulation problem is defined as one of determining the IA, IP, and IF functions for any given input image. We now have a number of different methods for computing AM-FM decompositions.

AM-FM decompositions provide for physically meaningful texture measurements. Usually, significant texture variations are captured in the frequency components. For single component cases, IF vectors are orthogonal to equi-intensity lines of an image, while the IF magnitude provides a measure of local frequency content. In (1), by using AM-FM components from different scales, we can produce IF vectors from different scales, at a pixel-level resolution [1,2].

Since AM-FM texture features are provided at a pixel-level resolution, AM-FM models can be used to segment texture images that are very difficult to model with the standard brightness-based methods [3]. On the other hand, using just histograms of the IF and IA, we can design effective content-based image retrieval systems using very short image feature vectors.

Some of the advantages of AM-FM models can be summarized in that: (i) they provide for a large number of physically meaningful texture features, over multiple scales, at a pixel-level resolution; (ii) we can reconstruct the image from the AM-FM decompositions; (iii) based on the target application, we can design for different AM-FM decompositions using different frequency coverage; and (iii) we have the recent development of very robust methods for AM-FM demodulation (see some recent examples in [1]).

We can extend AM-FM decompositions for representing videos using [4]:

$$I(x,y,t)=\sum_{n=1}^{N} a_n(x,y,t)\cos\phi_n(x,y,t) \qquad (2)$$

where each AM-FM function has been extended to be a function of both space and time. The original phase-based modeling approach was provided by Fleet and Jepson in [5] and was recently extended by Murray et al. in [4,6].

The comparison between an AM-FM reconstruction and the original image provides us with a method to better understand what AM-FM is measuring. For continuous-space image decompositions, AM-FM reconstruction examples can be found in [7], while [1,2] give several recent, robust multi-scale examples for both images and videos. AM-FM Transform examples were shown in [8], while multidimensional orthogonal FM transforms were demonstrated in [9].

An early example of the use of frequency-domain filtering to target a particular application can be found in the fingerprint examples in [10]. More recently, Ramachandran provided a tree-growth application, where inter-ring spacing was used to design filterbanks that cover a specific part of the spectrum, so as to recover tree ring and tree growth

M.S.Pattichis is with the Department of Electrical and Computer Engineering, University of New Mexico, Albuquerque, USA (e-mail: pattichis@ece.unm.edu).

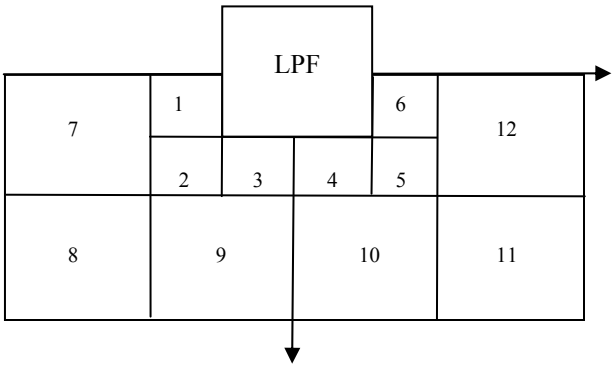

Fig. 1. Dyadic spectral coverage filterbank.

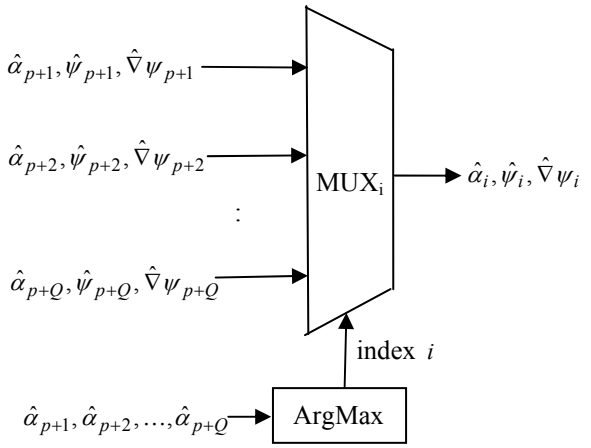

Fig. 2. Dominant Component Analysis (DCA) selecting the dominant AM-FM estimates from the collection of all estimates. Here, we have AM-FM estimates from each band (see Figs. 1 and 3).

structure from very noisy image inputs [11]. For general images, Gabor filterbank approaches were investigated by Havlicek in [12]. Similarly, for general images and videos, Murray introduced dyadic, multiscale decompositions in his dissertation [1].

Alternatively, AM-FM estimates can be obtained using an Energy Separation Algorithm (ESA) as described in [13-15]. Both ESA and Hilbert-based methods share the use of a filterbank prior to AM-FM demodulation. Furthermore, both methods extract estimates from a dominant component. For ESA, the dominant component is selected based on an energy criterion. In QEA, the dominant component is often selected based on IA estimates. More details on the methodology are given in Section II.

Due to space limitations, we will only provide details for the Hilbert-based methods. We provide a summary of biomedical imaging applications in Section III. Concluding remarks and possible future directions are given in Section IV.

II. Hilbert-Based AM-FM Methods

The basic, Hilbert-based AM-FM demodulation system is given in Figs 1-3. First, the real-valued input signal is "analytically" extended by removing all negative frequency components (see Figs. 1 and 3). The effect of this operation is to create a complex-valued signal of the form: $a(x,y)\exp[j\phi(x,y)]$. We then use a collection of bandpass filters to isolate the individual AM-FM components [12].

The basic assumption here is that different AM-FM components will be picked up by different bandpass filters, at the same image region. In other words, given any local image region, the assumption is that the corresponding AM-FM components will be separated by the use of different filters in the filterbank. The standard Gabor-based filterbank has dominated most of the studies on AM-FM decompositions (see [12]).

Here, we focus our attention on the new dyadic decompositions [1,2]. Our focus on the dyadic decomposition is based on its promise for significant improvements in AM-FM demodulation accuracy that is also derived from the fact that we have readily available methods for producing separable, optimal digital pass-band filters for implementing them.

A two-scale, dyadic filterbank coverage is shown in Fig. 1. Here, the high-frequency filters are numbered from 7 to 12, while the low-frequency filters are numbered from 1 to 6. The lowest frequencies are covered by a Low-Pass Filter (LPF). In this dyadic filterbank, each filter is designed using optimal 1-D filter design methods, allowing for very close approximations to ideal, bandpass filters. The filterbank can be easily extended to cover more scales, by applying the procedure iteratively. Alternatively, as in Wavelet theory, the same filterbank can be used to generate more scales by simply downsampling each filter output and re-applying the same two-scale filterbank.

Following each channel filter, we apply AM-FM demodulation to extract the individual AM-FM estimates from each bank. Here, we estimate AM-FM components using:

$$\hat{\alpha}_i(x,y) = \left| I_{AS}(x,y) * F_i(x,y) \right|$$

$$\hat{\psi}_i(x,y) = \arg\left[I_{AS}(x,y) * F_i(x,y) \right]$$

where $I_{AS}(x,y)$ denotes the extended analytic signal, $F_i(x,y)$ denotes the impulse response of the i-th filter, $\hat{\alpha}_i(x,y)$ denotes an IA estimate, and $\hat{\psi}_i(x,y)$ denotes an IP estimate.

A robust method for estimating the IF is based on considering [1,2]:

$$\frac{\partial \hat{\psi}_i}{\partial x}(x,y) = \frac{1}{\Delta x}\arccos\left(\frac{\bar{I}(x+\Delta x,y) + \bar{I}(x-\Delta x,y)}{2\bar{I}(x,y)} \right)$$

$$\frac{\partial \hat{\psi}_i}{\partial y}(x,y) = \frac{1}{\Delta y}\arccos\left(\frac{\bar{I}(x,y+\Delta y) + \bar{I}(x,y-\Delta y)}{2\bar{I}(x,y)} \right)$$

where $\bar{I}(x,y) = \exp[j\hat{\psi}_i(x,y)]$, and $\Delta x, \Delta y$ are selected so that they minimize the argument of the arc-cosine function. For the minimization, we simply select over a small integer number of pixels (1 to 4). We use the term Variable-Spacing Sequential Linear Phase (VS-SLP) to describe this method.

The VS-SLP is also related to an earlier method, termed the Quasi-Eigenfunction Approximation (QEA), used with Gabor filterbanks [12].

Following AM-FM demodulation at each channel filter, we reconstruct the AM-FM components by selecting AM-FM channel estimates with the largest IA estimate. The process, termed Dominant Component Analysis (DCA) [12], is applied at every pixel (see Figs. 2). For multi-scale decomposition, we select estimates by scale [1].

III. BIOMEDICAL IMAGE APPLICATIONS

We provide a selected list of Biomedical imaging applications in Table I. For a summary of the AM-FM methods we refer to the discussion in Section II.

In one of the earlier applications in electron microcopy, a simple Bayesian method using the IA and the IF was used, in conjunction with morphological filtering to provide segmentations of different abnormalities over 26 images [3]. Elshinawy et al [18] demonstrated the reconstruction of breast cancer images using AM-FM components.

We also have a number of medical applications based on energy operators. Boudraa et al [19] introduced a new cross-energy operator and used the operator to demonstrate the functional segmentation of dynamic nuclear images. Maragos et al. provide an important application in [16], where AM-FM models are used for improving Doppler ultrasound resolution. For the first time, vector-valued based AM-FM demodulation is given in [17].

In Murray et al. [6], Hilbet-based AM-FM methods were used for providing accurate motion estimation. More recently, in 2008, Murray et al. [20] and Agurto et al. [21] demonstrated the use of multi-scale AM-FM models for retinal image analysis. Using 18 images from four different risk levels, the authors showed that AM-FM methods provided excellent separations with ROC areas ranging from 0.93 (0 vs 1) to 0.99 (0 vs 3) [21].

IV. CONCLUSIONS AND FUTURE WORK

AM-FM methods provide for great opportunities for application in Biomedical Imaging. Over the years, the methods have matured to the point that we now have robust AM-FM demodulation methods over multiple scales.

Future work can focus on the development of new filterbanks that will be specifically tuned to specific applications. The use of different, user-defined scales for specific applications is also a very promising area. The large number of generated AM-FM features requires the future study of feature selection methods, as well as methods for describing the covariance structure among the different features.

REFERENCES

[1] Victor Manuel Murray Herrera, "AM-FM methods for image and video processing," Ph.D. dissertation, University of New Mexico, 2008.

[2] V. Murray, P. Rodriguez V., and M.S. Pattichis, "Multi-scale AM-FM demodulation and reconstruction methods with improved accuracy," in revision, *IEEE Trans. on Image Processing.*

[3] M.S. Pattichis, C.S. Pattichis, M. Avraam, A.C. Bovik, and K. Kyriakou, "AM-FM Texture Segmentation in Electron Microscopic Muscle Imaging," *IEEE Trans. on Medical Imaging*, vol. 19, no. 12, pp. 1253-1258, Dec. 2000.

[4] V. Murray and M.S. Pattichis, "AM-FM Demodulation Methods for Reconstruction, Analysis and Motion Estimation in Video signals," *2008 IEEE Southwest Symposium on Image Analysis and Interpretation*, Santa Fe, New Mexico, pp. 17-20, Mar., 2008.

[5] D.J. Fleet and A.D. Jepson, "Computation of component image velocity from local phase information," *International Journal of Computer Vision*, vol. 5, no. 1, pp. 77-104, 1990.

[6] V. Murray, V., S.E. Murillo, M.S. Pattichis, C.P. Loizou, C.S. Pattichis, E. Kyriacou, E. and A.N. Nicolaides, "An AM-FM model for Motion Estimation in Atherosclerotic Plaque Videos," invited in the *41st Asilomar Conference on Signals, Systems, and Computers, Asilomar Hotel and Conference Grounds, Pacific Grove*, CA, pp. 746-750, Nov. 4-7, 2007.

[7] J.P. Havlicek, P.C. Tay, and A.C. Bovik, "AM-FM Image Models: Fundamentatl Techniques and Emerging Trends," in *Handbook of Image and Video Processing*, 2nd ed, A.C. Bovik, ed., Elsevier Academic Press, Burlington, pp. 377-395, MA, 2005.

[8] M.S. Pattichis and A.C. Bovik, "AM-FM Expansions for Images," in *Proc. European Signal Processing Conf.*, Trieste, Italy, Sept. 1996.

[9] M.S. Pattichis, A.C. Bovik and J.W. Havlicek, "Multidimensional Orthogonal FM Transforms," *IEEE Trans. on Image Processing*, vol. 10, no. 3, pp. 448-464, March 2001.

[10] M.S. Pattichis, G. Panayi, A.C. Bovik, and H. Shun-Pin, "Fingerprint classification using an AM-FM model," *IEEE Trans. on Image Processing*, vol. 10, no. 6, pp. 951-954, June 2001.

[11] J. Ramachandran, "Image analysis of wood core using instantaneous wavelength and frequency modulation," Ph.D. dissertation, University of New Mexico, 2008.

[12] J. P. Havlicek, "AM-FM image models," Ph.D. dissertation, The University of Texas at Austing, 1996.

[13] P. Maragos, J.F. Kaiser, and T.F. Quatieri, "On amplitude and frequency demodulation using energy operators," *IEEE Trans. on Signal Processing*, vol. 41, no. 4, pp. 1532-1550, April 1993.

[14] P. Maragos, J.F. Kaiser, and T.F. Quatieri, "Energy Separation in Signal Modulations with Application to Speech Analysis," *IEEE Trans. on Signal Processing*, vol. 41, no. 10, pp. 3024-3051, October 1993.

[15] P. Maragos and A.C. Bovik, "Image Demodulation using Multidimensional Energy Separation," *J. Opt. Soc. Am. A.*, vol. 12, no. 9, pp. 1867-1876, September 1995.

[16] P. Maragos, T. Loupas and V. Pitsikalis, "On Improving Doppler Ultrasound Spectroscopy with Instantaneous Multiband Energy Separation," in *Proc. IEEE 14th International Conference on Digital Signal Processing* (*DSP-2002*), Santorini, Greece, July 2002.

[17] E. Alexandatou, A. Sofou, H. Papasaika, P. Maragos, D. Yova, and N. Kavatzas, "Computer Vision Algorithms in DNA ploidy image analysis," in *Proc. of the SPIE Imaging, Manipulation, and Analysis of Biomolecules, Celss, and Tissues IV*, vol. 6088, pp. 180-190, 2006.

[18] Y.M. Elshinaway, Z. Jianchao, B. S.C Lo and M.F. Chouikha, "Breast cancer detection in mammogram with AM-FM modeling and Gabor filtering," in *Proc. 7th International Conference on Signal Processing* (ICSP), Beijing, China, vol. 3, pp. 2564-2567, Sept. 2004.

[19] A. Bourdraa, J. Cexus, and H. Zaidi, "Functional segmentation of dynamic nuclear images by cross-ψ_B-energy operator," *Computer Methods and Programs in Biomedicine*, vol. 84, pp. 146-152, 2006.

[20] V. Murray, M.S. Pattichis, and P. Soliz, "Analysis Methods for Retinal Image Characterization," invited in *Proc. 42nd Asilomar Conference on Signals, Systems and Computers*, 5 pages, Oct. 26-29, 2008.

[21] C. Agurto, S. Murillo, V. Murray, M.S. Pattichis, S. Russell, M. Abramoff, and P. Soliz, "Detection and Phenotyping of Retinal Disease using AM-FM Processing for Feature Extraction," invited in Proc. 42nd Asilomar Conference on Signals, Systems and Computers, 5 pages, Oct. 26-29, 2008.

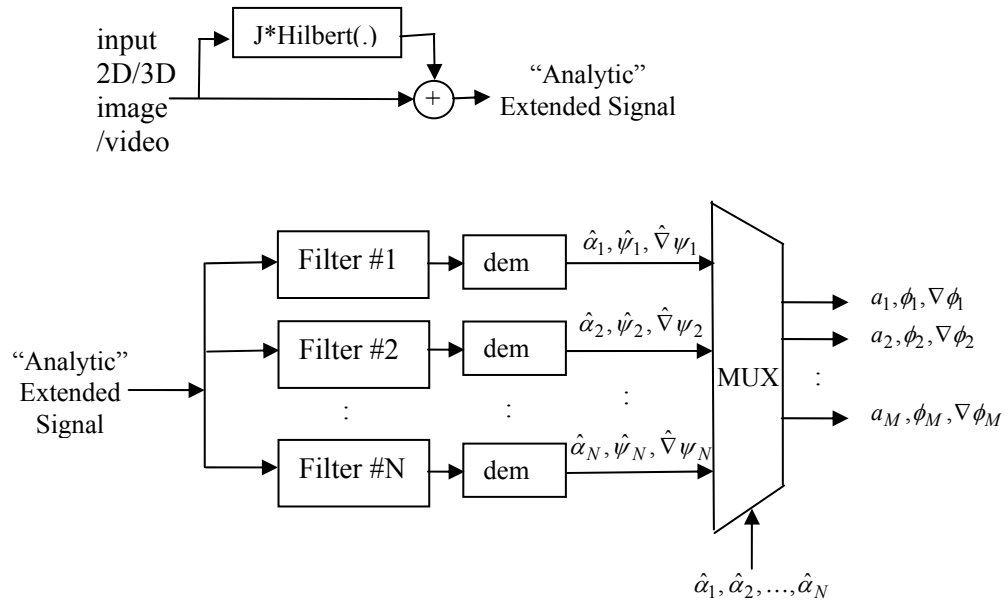

Fig. 3. Hilbert-based AM-FM Demodulation System for Images and Video. The input signal is used to produce a complex-valued "analytic" signal. The complex "analytic signal is fed to a collection of bandpass filters for demodulation (see text for details).

TABLE I. SELECT LIST OF AM-FM APPLICATIONS IN BIOMEDICAL IMAGING.

Author	**Filterbank**	**AM-FM Demodulation Method**	**Medical Application**
Pattichis et al. 2000 [3]	Gabor filterbank	QEA	Electron microscopy image segmentation
Maragos et al. 2002 [16]	1-D Gabor filterbank	ESA	Doppler ultrasound spectroscopy resolution
Elshinawy et al. 2004 [18]	Gabor filterbank	QEA and continuous-space demodulation	Demonstrated AM-FM reconstructions of breast cancer images
Boudraa et al. 2006 [19]		Cross Ψ_B energy operator	Nuclear cardiac sequences for one normal and four abnormal cases
Alexandratou et al. [17]	Gabor filterbank	Vector-valued ESA for color images	Ploidy image analysis (cancer).
Murray et al, 2007 [6]	Dyadic 3D filterbank	QEA + new AM and FM motion estimation	Motion Estimation for Atherosclerotic Plaque videos compared against other Phased-based method
Murray et al [20] and Agurto et al [21], 2008	Dyadic 2D filterbank	New VS-SQP method	Retinal image analysis.